pharmaceuticals

MDPI

Article

Phytochemical Investigation of *Juncus hybridus*: Truxinic Acid Sucrose Diesters and α-Glucosidase Inhibitory Activity

Anita Barta [1,2], Gábor Girst [1], Judit Hohmann [1,2] and Andrea Vasas [1,2,*]

[1] Institute of Pharmacognosy, University of Szeged, Eötvös Str. 6, 6720 Szeged, Hungary; bartaanita96@gmail.com (A.B.); girst.gabor.02@szte.hu (G.G.); hohmann.judit@szte.hu (J.H.)
[2] HUN-REN–USZ Biologically Active Natural Products Research Group, University of Szeged, Eötvös Str. 6, 6720 Szeged, Hungary
* Correspondence: vasas.andrea@szte.hu; Tel.: +36-62546451

Abstract

Background/Objectives: Truxinic acid derivatives, particularly their glycosylated forms, are rare natural products with a limited distribution in the plant kingdom. As part of our ongoing phytochemical investigations of Juncaceae species, the secondary metabolites of *Juncus hybridus* were investigated. **Methods:** Chromatographic separation of the methanolic extract resulted in the isolation of fifteen compounds, including truxinic acid derivatives, phenanthrenes, flavonoids, other phenolic compounds, and megastigmanes. Their structures were elucidated by extensive spectroscopic analyses, including 1D and 2D NMR spectroscopy and high-resolution mass spectrometry (HR-MS). **Results:** Two compounds, junhybridins A and B, were identified as new truxinic acid sucrose diesters. This study provides a comprehensive report of the phytochemical composition of *J. hybridus*. The identification of two new truxinic acid derivatives further expands the known chemical diversity of the Juncaceae family. Seven selected compounds were evaluated for their α-glucosidase inhibitory activity. Among them, luteolin displayed the strongest inhibition, with an IC_{50} value of 5.91 μM, while juncusol also exhibited considerable activity. **Conclusions:** These findings expand the chemotaxonomic knowledge of the Juncaceae family and identify *J. hybridus* as an unexpected source of rare glycosylated truxinic acid derivatives.

Keywords: *Juncus hybridus*; Juncaceae; truxinic acids; phenanthrenes; megastigmanes; α-glucosidase inhibitory activity

1. Introduction

Truxillic acids, truxinic acids, and their derivatives are belonging to a class of interesting cyclobutene-containing natural products with unique structural features. These compounds are formed from two cinnamic acid units linked via C–C bonds between the C-7/C-7′ and C-8/C-8′ carbons of the monomers. Depending on the stereochemistry of the precursor cinnamic acid, *cis*- or *trans*-cinnamic acid undergoes photochemically induced [2 + 2] cycloaddition according to the Woodward–Hoffmann rules, yielding truxillic acid or truxinic acid derivatives through head-to-head or head-to-tail coupling, respectively [1,2]. Depending on the orientation of the phenyl and carboxyl groups relative to the cyclobutane ring plane, truxillic acids have six stereocentres, whereas truxinic acids can exist as eight possible stereoisomers [3]. Truxillic and truxinic acids and their 4,4′-hydroxylated derivatives are commonly conjugated with various substituents through carbon, oxygen, and nitrogen atoms [2]. To date, glycosylated derivatives have been reported exclusively among truxinic acid derivatives, with the sugar moieties linked through *O*-glycosidic bonds.

Check for updates

Academic Editor: Grażyna Zgórka

Received: 2 September 2026
Revised: 16 October 2026
Accepted: 20 October 2026
Published: 22 October 2026

Copyright: © 2026 by the authors. Licensee MDPI, Basel, Switzerland. This article is an open access article distributed under the terms and conditions of the Creative Commons Attribution (CC BY) license.

To the best of our knowledge, only ten glycosylated truxinic acid derivatives have been isolated from natural sources, originating from species of the Poaceae, Asteraceae, and Euphorbiaceae families [4–10]. Truxinic acid derivatives have been reported to possess various biological activities, including anti-inflammatory [5,10], antidiabetic [11,12], and aldose reductase inhibitory [13] effects.

Juncaceae species, especially those belonging to the genera *Juncus* and *Luzula*, have attracted considerable phytochemical and pharmacological interest due to their remarkable ability to biosynthesize structurally diverse phenolic secondary metabolites, e.g., phenanthrenes, phenolic acids, and flavonoids [14]. Phenanthrenes represent one of the most characteristic and biologically important classes of compounds identified in Juncaceae [15]. Although phenanthrenes occur only sporadically in the plant kingdom, Juncaceae species are considered one of the richest natural sources of these metabolites. To date, more than one hundred phenanthrenes have been identified from members of the family, including mono- and diphenanthrenes, as well as glycosylated derivatives [15,16]. A distinctive chemotaxonomic feature of Juncaceae phenanthrenes is the frequent occurrence of vinyl-substituted skeletons, a structural motif rarely encountered outside this plant family [17].

The pharmacological potential of Juncaceae metabolites has been extensively investigated over the past three decades. Phenanthrene derivatives isolated from *Juncus* species have exhibited significant antiproliferative and cytotoxic activities against several human cancer cell lines, including HeLa, MCF-7, A2780, and T-47D cells [18]. In particular, dimeric phenanthrenes often display greater biological activity than their monomeric analogues, suggesting that molecular dimerization may enhance interactions with biological targets [19,20]. Several compounds have also demonstrated antimicrobial activity against Gram-positive bacteria, fungi, and herpes simplex virus type 2, while others exhibited anti-inflammatory, antioxidant, anxiolytic, sedative, spasmolytic, and antibiofilm properties [15,18]. Among the known Juncaceae metabolites, dehydrojuncusol has emerged as one of the most extensively studied compounds due to its broad spectrum of biological activities, including antimicrobial and antiproliferative effects [21].

α-Glucosidase inhibitors (AGIs) reduce postprandial glucose by slowing intestinal carbohydrate hydrolysis, a validated therapeutic strategy for type 2 diabetes, and natural products contribute a diverse array of AGIs [22]. Previous research has explored the antidiabetic properties of truxillic and truxinic acids, along with their derivatives, through the interaction with key metabolic targets [e.g., peroxisome proliferator-activated receptor (PPARγ) activation, fatty acid binding protein (FABP) inhibition] to regulate blood sugar, reduce insulin resistance, and treat diabetes [23–25]. Moreover, some phenanthrenes have also shown AGI activity [26]. Natural products offer a rich source of AGIs, including flavonoids, phenanthrenes, bibenzyls, and related glycosides [27,28].

In continuation of our work aiming at the isolation of biologically active compounds from Juncaceae species, *Juncus hybridus* (*J. hybridus*) was selected for phytochemical investigation [29]. The isolated compounds were evaluated for their AGI activity with the goal of identifying natural products with potential relevance to antidiabetic drug discovery.

2. Results and Discussion

Air-dried and ground whole plant of *J. hybridus* was extracted with methanol at room temperature. After evaporation, the extract was dissolved in 50% aqueous methanol and subjected to solvent–solvent partitioning with *n*-hexane, chloroform, and ethyl acetate. The chloroform and ethyl acetate phases were fractionated by vacuum liquid chromatography (VLC) and purified by preparative thin-layer chromatography (prep. TLC) and high-performance liquid chromatography (HPLC), yielding 15 compounds. The struc-

tures were elucidated by extensive spectroscopic analysis, including NMR and HRESIMS measurements, together with comparison of the spectral data with literature values.

2.1. Structure Elucidation of the Compounds

Compound **1** (junhybridin A) was obtained as a yellow oily solid. Its molecular formula was determined as $C_{34}H_{40}O_{18}$ by (+)-HRESIMS analysis (*m*/*z* 754.2539 $[M + NH_3 + H]^+$, calcd for $C_{34}H_{44}O_{18}N^+$ 754.2553, $\Delta = -1.9$ ppm) (Figure S1). In the ^{1}H NMR spectrum (Table 1, Figure S2), two sets of ABX-coupled spin systems [δ_H 6.45 (1H, d, J = 1.6 Hz, H-2), 6.61 (1H, d, J = 8.2 Hz, H-5), 6.55 (1H, dd, J = 1.6 and 8.2 Hz, H-6), 6.42 (1H, d, J = 1.5 Hz, H-2′), 6.59 (1H, d, J = 8.3 Hz, H-5′), 6.53 (1H, dd, J = 1.5 and 8.3 Hz, H-6′)], two methoxy groups [δ_H 3.64 (3H, s, OCH_3-3), 3.62 (3H, s, OCH_3-3′)], an acetyl-methyl [δ_H 1.90 (3H, s, $COCH_3$-3‴)] and sugar moieties were observed. In the ^{13}C NMR JMOD (*J*-modulated spin-echo experiment) spectrum, 34 carbon signals were detected, which were categorized based on their HSQC correlations and chemical shifts into three methyls, three aliphatic methylenes, eighteen methines and ten non-protonated carbons (Table 1, Figures S3 and S5).

Table 1. ^{1}H (500 MHz) and ^{13}C NMR (125 MHz) data of compounds **1** and **2** in methanol-d_4 [500 MHz (^{1}H), 125 MHz (^{13}C), δ ppm].

	1		**2**	
Position	**δ_C, Type**	**δ_H (J in Hz)**	**δ_C, Type**	**δ_H (J in Hz)**
1	131.6, C		132.0, C	
2	113.5, CH	6.45 d (1.6)	113.4, CH	6.45 d (1.7)
3	148.5, C		148.7, C	
4	146.1, C		146.1, C	
5	115.7, CH	6.61 d (8.2)	115.7, CH	6.60 d (8.0)
6	121.8, CH	6.55 dd (8.2, 1.6)	121.9, CH	6.55 dd (8.0, 1.7)
7	44.6, CH	4.12 dd (9.6, 5.5)	44.7, CH	4.09 dd (9.1, 5.1)
8	46.2, CH	3.84 dd (10.9, 5.5)	46.4, CH	3.82 m
9	175.4, C		175.6, C	
3-OCH_3	56.4, CH_3	3.64 s	56.4, CH_3	3.64 s
1′	131.9, C		131.7, C	
2′	113.2, CH	6.42 d (1.5)	113.2, CH	6.42 d (1.8)
3′	148.7, C		148.5, C	
4′	146.0, C		145.9, C	
5′	115.5, CH	6.59 d (8.3)	115.5, CH	6.58 d (8.0)
6′	121.8, CH	6.53 dd (8.3, 1.5)	121.7, CH	6.53 dd (8.0, 1.8)
7′	45.4, CH	4.36 dd (9.7, 9.2)	45.4, CH	4.38 m
8′	45.1, CH	4.31 dd (10.9-, 9.2)	45.0, CH	4.39 m
9′	172.8, C		173.1, C	
3′-OCH_3	56.4, CH_3	3.62 s	56.4, CH_3	3.62 s
1″ Glc	94.4, CH	5.49 d (3.5)	94.5, CH	5.46 d (3.6)
2″	73.6, CH	3.49 dd (9.4, 3.5)	73.7, CH	3.49 dd (9.5, 3.6)
3″	75.2, CH	3.76 t (9.4)	75.4, CH	3.76 t (9.5)
4″	71.6, CH	3.40 t (9.4)	71.4, CH	3.48 t (9.5)
5″	72.1, CH	4.33 m	74.1, CH	4.19 m
6″	65.2, CH_2	4.50 dd (11.8, 1.8) 4.24 dd (11.8, 5.2)	62.8, CH_2	3.90 dd (11.8, 1.8) 3.84 dd (11.8, 5.2)
1‴ Fr	63.7, CH_2	3.82 s (2H)	63.7, CH_2	3.82 m
2‴	109.8, C		109.8, C	
3‴	79.6, CH	4.90 s	79.6, CH	4.90 s
4‴	75.6, CH	4.40 m	75.6, CH	4.41 s
5‴	89.3, CH	4.17 br s	89.3, CH	4.17 br s
6‴	65.5, CH_2	5.04 d (12.5) 4.15 m	65.4, CH_2	5.01 d (12.3) 4.15 dd (12.3, 1.9)
3‴-AcCO	173.0, C		-	
3‴-$AcCH_3$	20.7, CH_3	1.90 s	-	

The presence of two 3-methoxy-4-hydroxyphenyl groups was confirmed by twelve olefinic carbons (δ_C 113.5–148.7) and two methoxy carbons (δ_C 2 × 56.4). ^{1}H–^{1}H-COSY correlations were observed between δ_H 6.61 d and 6.55 dd (H-5/H-6) and between δ_H 6.59 d and 6.53 dd (H-5′/H-6′) and HMBC cross-peaks of H-2 (δ_H 6.45 d) and H-6 (δ_H 6.55 dd) with C-4 (δ_C 146.1), H-5 (δ_H 6.61 d) and OCH_3-3 (δ_H 3.64 s) with C-3 (δ_C 148.5), H-2′ (δ_H 6.42 d) and H-6′ (δ_H 6.53 dd) with C-4′ (δ_C 146.0) and H-5′ (δ_H 6.59 d) and OCH_3-3′ (δ_H 3.62 s) with C-3′ (δ_C 148.7) (Figures 1, S4, S6 and S7). Four aliphatic methines [δ_C 44.6 (C-7), 46.2 (C-8), 45.4 (C-7′), 45.1 (C-8′)] and ^{1}H–^{1}H-COSY cross-peaks of δ_H 4.12 dd, 3.84 dd, 4.36 t and 4.31 t (H-7/H-8/H-7′/H-8′) were attributed to a cyclobutane ring. HMBC correlations between H-7 (δ_H 4.12 dd) and C-1 (δ_C 131.6), C-2 (δ_C 113.5) and C-6 (δ_C 121.8), H-7′ (δ_H 4.36 t) and C-1′ (δ_C 131.9), and C-2′ (δ_C 113.2) and C-6′ (δ_C 121.8) indicated that two 3-methoxy-4-hydroxylphenyl groups were correspondingly attached to C-7 and C-7′. Two carboxyl groups located at C-8 and C-8′ established the truxinic acid skeleton, which was further supported by HMBC correlations between H-7 (δ_H 4.12 dd) and C-9 (δ_C 175.4), and H-7′ (δ_H 4.36 t) and C-9′ (δ_C 172.8) (Figures 1, S6 and S7).

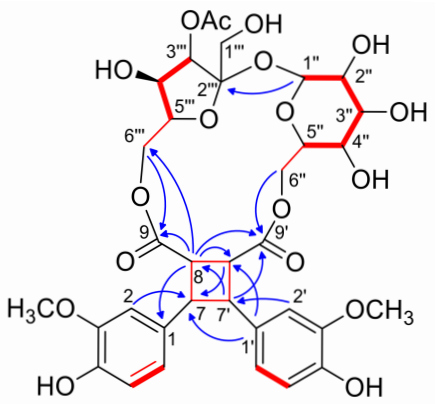


Figure 1. ^{1}H–^{1}H COSY (—) and key HMBC (H↔C) correlations of compound **1**.

The remaining twelve oxygenated carbons (δ_C 63.7–109.8) were assigned to a disaccharide moiety. Assignments of the disaccharide backbone were elucidated by two sets of distinct ^{1}H–^{1}H-COSY cross-peaks between δ_H 5.49 d, 3.49 dd, 3.76 t, 3.40 t, 4.33 m, 4.24 dd and 4.50 dd (H-1″/H-2″/H-3″/H-4″/H-5″/H_2-6″) and between δ_H 4.90 s, 4.40 m, 4.17 br s, 4.15 m and 5.04 d (H-3‴/H-4‴/H-5‴/H_2-6‴) (Figure S4). The characteristic anomeric doublet signal at 5.49 with a small coupling constant (d, J = 3.5 Hz, H-1′) suggested an α-glucopyranoside unit which is linked to a fructopyranose, based on the HMBC correlation of Glc H-1″ and Fru C-2‴. The chemical shifts of the sucrose moiety were in good agreement with those reported for helonioside B [30]. Moreover, alkaline hydrolysis of **1** gave sucrose [α-D-Glc-(1→2)-β-D-Fru], which was identified by co-TLC and comparison of the optical rotation data with those of an authentic sample.

Diester linkages were established between C-9 and C-6‴ and between C-9′ and C-6″, which were confirmed by HMBC correlations between H_2-6″ (δ_H 4.24 dd) and C-9′ (δ_C 172.8), and H-6‴ (δ_H 4.15 m, 5.04 d) and C-9 (δ_C 175.4). Based on the HMBC correlations of the acetyl methyl group (δ_H 1.90 s) and H-3‴ (δ_H 4.90 s) with acetyl carbonyl (δ_C 173.0), the acetyl group was placed at the C-3‴ position (Figures 1, S6 and S7).

Finally, stereogenic centers at the truxinic acid backbone were elucidated by the NOESY spectrum (Figures 2 and S8). Overhauser effects were detected between H-8/H-2 and H-6, and H-8′/H-2′ and H-6′, indicating *trans*-orientations between H-7/H-8 and H-7′/H-8′. The NOESY correlation between H-7/H-7′ and H-8/H-8′ indicated *cis*-orientations of H-7/H-7′ and H-8/H-8′. The coupling constants of H-7, H-7′, H-8, and H-8′ were in good agreement with those of trigohonbanoside A [9]. Thus, the relative configuration of the truxinic acid

backbone is 7*α*,8*β*,7′*α*,8′*β*. Consequently, the structure of compound **1** was established as presented in Figure 1 and was named as junhybridin A.

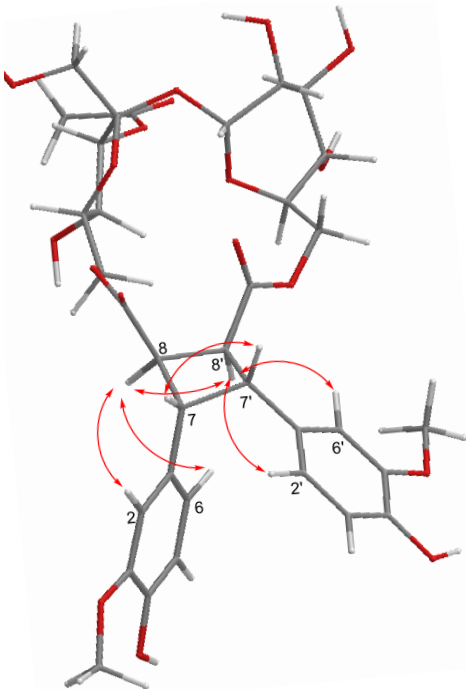


Figure 2. Key NOESY correlations (↔) of compound **1**.

Compound **1** differs from trigohonbanoside A, a truxinic acid sucrose diester previously isolated from *Trigonostemon honbaensis* (Euphorbiaceae), in having an acetate group instead of a hydroxyl group at C-3‴ [9].

Compound **2** (junhybridin B) was obtained as a pale yellow syrup with molecular formula of $C_{32}H_{38}O_{17}$, deduced from its (+)-HRESIMS data (*m*/*z* 712.2443 [M + NH_3 + H]$^+$, calcd for $C_{32}H_{42}O_{17}N^+$, 712.2452, Δ = −1.3 ppm) (Figure S9). Analysis of the 1D and 2D NMR data revealed the same esterified truxinic acid skeleton as in compound **1**, bearing 3-methoxy-4-hydroxy-substituted phenyl groups and glycosylated with one glucose and one fructose unit (Table 1, Figures S10–S15). The glucose and fructose units formed a sucrose moiety, as indicated by the HMBC correlation of H-1″ (δ_H 5.46, glucose) and C-2‴ (δ_C 109.8, fructose) (Figures S14 and S15). Furthermore, alkaline hydrolysis of **2** afforded a product that was identified as sucrose through a comparison of its optical rotation and co-TLC data with an authentic sample. Unlike in compound **1**, the sucrose moiety was linked to the truxinic acid skeleton through the fructose unit; both carboxyl groups are connected to the fructose part in position C-3‴ and C-6‴. This assignment was confirmed by the HMBC cross-peaks between H_2-6‴ (δ_H 5.01 d, 4.15 dd) and C-9 (δ_C 175.6) and H-3‴ (δ_H 4.90) and C-9′ (δ_C 173.1). The relative configuration of compound **2** was found to be identical to that of **1**, as evidenced by the NOESY correlations between H-2/H-8, H-6/H-8, H-2′/H-8′, and H-6′/H-8′ and the coupling constants of H-7 and H-8 (Figure S16). According to the above evidence, the structure of compound **2** was elucidated as shown in Figure 3 and was named junhybridin B.

Junhybridins A and B (**1** and **2**) therefore belong to the rare group of sucrose-substituted truxinic acid esters. Sucrose-containing truxinic acid esters are exceptionally rare in the plant kingdom, with only ten such compounds having been reported to date [2,9,10]. In four of these compounds, truxinic acid forms a diester exclusively with the fructose moiety at the 1,3- or 3,6-positions (*Coix*, *Avena*, and *Imperata* metabolites), whereas in the remaining six compounds, truxinic acid esterifies both glucose and fructose at the

6,6′-positions (*Trigonostemon* and *Bidens* metabolites). Junhybridin B (**2**) belongs to the former group, with esterification at the 3,6-positions of fructose, whereas junhybridin A (**1**) represents the latter structural pattern, with the two ester groups involving glucose and fructose. Both compounds were isolated in amounts of approximately 300 mg each, corresponding to an isolated yield of approximately 0.09% (*w*/*w*) based on the dry weight of the starting plant material. Their occurrence is particularly noteworthy because truxinic acid derivatives had not previously been reported from Juncaceae species.

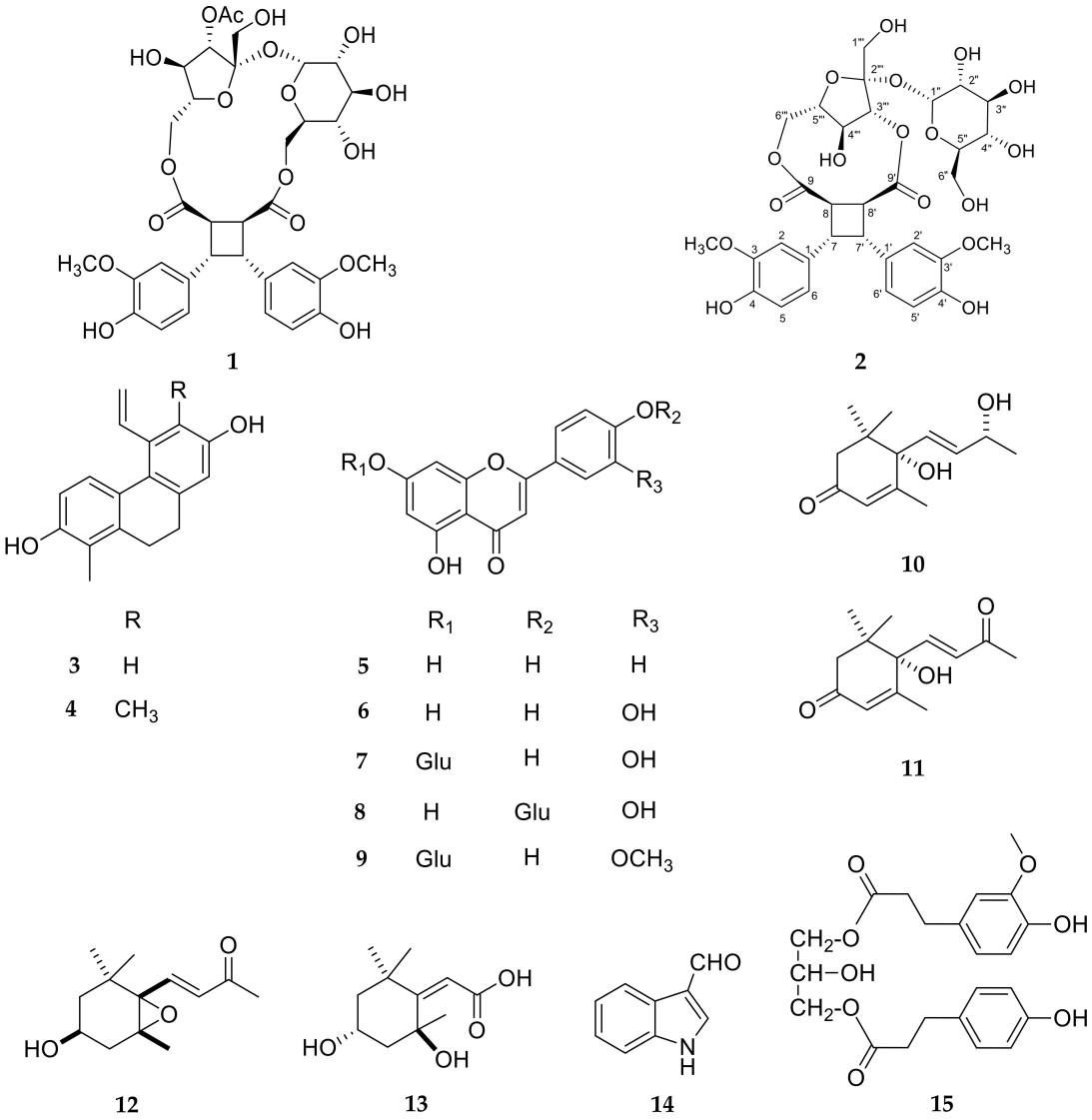


Figure 3. Structure of the isolated compounds (**1**–**15**).

Although phenanthrenes are the main special metabolites of Juncaceae species from phytochemical, pharmacological, and chemotaxonomical points of view, only effusol (**3**) and juncusol (**4**) could be identified from *J. hybridus* [31]. In addition to truxinic acids and phenanthrenes, apigenin (**5**) [32], luteolin (**6**) [32], luteolin-7-*O*-*β*-D-glucoside (**7**) [33], luteolin-4′-*O*-*β*-D-glucoside (**8**) [33], chrysoeriol 7-*O*-*β*-D-glucoside (**9**) [34], (+)-(6*S*,9*R*)-vomifoliol (**10**) [35], dehydrovomifoliol (**11**) [36], 6*α*-epoxy-7-megastigmen-9-one (**12**) [37], (*Z*)-2-(2,4-dihydroxy-2,6,6-trimethylcyclohexylidene)acetic acid (**13**) [38], 1*H*-indole-3-carboxaldehyde (**14**) and 1-*O*-feruloyl-3-*O*-*p*-coumaroylglycerol (**15**) [39] were isolated from this plant (Figure 3). The NMR data of **13** were measured in a different solvent than previously reported; the data are provided in the Materials and Methods Section.

The relatively low abundance and diversity of phenanthrenes observed in the investigated plant may be related to environmental or developmental factors; however, this possibility remains hypothetical, as the present study did not experimentally compare plants exposed to different biotic or abiotic conditions. Phenanthrene accumulation in Juncaceae may be influenced by external factors, including biotic stress such as microbial infection, as well as seasonal variation, tissue specificity, developmental stage, and other ecological conditions. Comparative analyses of *J. hybridus* material collected from different environments or developmental stages, or obtained under controlled biotic and abiotic conditions, would be valuable for testing this hypothesis.

2.2. Pharmacological Investigation

The α-glucosidase inhibitory (AGI) activity of phenolic compounds, among them truxinic acid derivatives (**1** and **2**), phenanthrenes (**3** and **4**), and flavonoids (**5**, **6**, and **9**), was screened at two concentrations (100 and 10 µM), using acarbose, the most widely prescribed drug, as a positive control. IC_{50} values were only determined where significant inhibition was observed even at the lower concentration. The results are shown in Table 2. Among the isolated compounds, luteolin (**6**) exhibited the strongest inhibitory effect against AG, with an IC_{50} value of 5.91 µM. Although the activity of juncusol (**4**) was lower than that of luteolin (**6**), it still demonstrated considerable inhibition of AG activity, reducing enzyme activity by 75.6% at a concentration of 100 µM. At 100 µM, effusol (**3**), junhybridin B (**2**), chrysoeriol 7-*O*-*β*-D-glucoside (**9**), junhybridin A (**1**), and apigenin (**5**) inhibited α-glucosidase by 55.0%, 46.4%, 45.5%, 37.8%, and 35.1%, respectively. The IC_{50} value of acarbose, which varies considerably across the literature, was determined to be 0.00180 µM, in the same order of magnitude as the values reported in Refs [40–43]. It should be noted that AGI activity and IC_{50} values are strongly dependent on the experimental conditions, including the enzyme source, substrate, incubation conditions, and analytical method. Therefore, direct quantitative comparisons of IC_{50} values obtained in different studies should be interpreted with caution. In the present study, the comparison between the isolated compounds and acarbose is based on their activities determined under identical experimental conditions, making the relative differences observed within this assay more informative than comparisons with IC_{50} values reported in the literature.

Table 2. α-Glucosidase inhibitory activity of compounds **1**–**6** and **9**.

Compound	Inhibition % at 100 µM		Inhibition % at 10 µM			
	Mean	SD	Mean	SD	IC_{50} (µM)	95% CI
1	37.8	4.2	3.5	2.8		
2	46.4	2.6	12.6	7.0		
3	55.0	5.3	−1.5	5.2		
4	75.6	2.8	9.7	5.0		
5	35.1	3.7	−2.2	6.7		
6	94.7	3.6	50.1	2.6	5.91	4.72 to 7.12
9	45.5	8.4	5.8	5.2		
acarbose	90.4	1.9	89.6	1.5	0.00180	0.0016 to 0.0020

Among the isolated phenolic constituents, luteolin (**6**) was by far the most potent AGI, whereas all other compounds showed measurable inhibition under the applied assay conditions. The observed activity of luteolin (**6**) is consistent with previous mechanistic

studies, which have suggested that luteolin (**6**) can inhibit α-glucosidase through reversible non-competitive or mixed inhibition mechanisms involving hydrophobic interactions and hydrogen bonding with residues located near the catalytic pocket, accompanied by conformational changes in the enzyme [27,44,45]. The pronounced activity of luteolin (**6**) may be related to its structural characteristics. Previous studies on flavonoid structure–activity relationships (SARs) have suggested that α-glucosidase inhibition is favored by the flavone scaffold containing the C-2–C-3 double bond conjugated with the 4-oxo group, which maintains molecular planarity and facilitates π–π interactions with aromatic residues within the enzyme. Furthermore, the hydroxylation pattern is critical, with the catechol moiety in ring B (3′,4′-dihydroxylation) and the presence of the 5-hydroxyl group substantially enhancing binding affinity through hydrogen bond formation [46,47]. These structural features provide a plausible explanation for the relatively strong activity of luteolin (**6**) observed in the present assay. However, the comparison of only three flavonoids in the present study does not allow a definitive structure–activity relationship to be established. The lower activity observed for apigenin (**5**) is consistent with these previously reported SAR trends; however, the present data alone are insufficient to establish the contribution of the 3′-hydroxyl group in ring B to α-glucosidase inhibition. Previous comparative studies have associated the removal of this hydroxyl group with reduced AGI activity, highlighting the importance of this substitution for enzyme binding [48]. Accordingly, the relatively weak inhibition observed for apigenin (**5**) in the present study is fully consistent with published SAR analyses. The flavonoid glycoside chrysoeriol 7-*O*-*β*-D-glucoside (**9**) also displayed measurable inhibitory activity. Glycosylation is generally considered detrimental to AG inhibition because the attached sugar increases molecular size and polarity while reducing the accessibility of the flavonoid core to the enzyme binding pocket. In many flavonoid series, aglycones exhibit considerably stronger inhibitory activity than their corresponding glycosides, particularly when glycosylation occurs at positions involved in hydrogen bonding or sterically interferes with enzyme binding [48]. The present findings therefore agree well with previous reports showing that glycosylation frequently attenuates AGI potency, although the magnitude of this effect depends on both the sugar residue and its attachment site.

The phenanthrene derivative juncusol (**4**) produced 75.6% inhibition at 100 μM, indicating a moderate inhibitory potential. Compared with flavonoids, relatively little information is available concerning the AGI activity of phenanthrenes [26]. Nevertheless, their rigid polycyclic aromatic scaffold may facilitate hydrophobic interactions and π-stacking within the enzyme binding pocket, which could explain the measurable inhibitory activity observed here. The lower activity of effusol (**3**), despite belonging to the same structural class, suggests that subtle differences in hydroxylation pattern (missing *ortho*-dihydroxy moiety), substitution, or dimerization substantially influence enzyme affinity. Since only a limited number of naturally occurring phenanthrenes have been evaluated against AG, the current results contribute additional evidence supporting this compound class as a promising, although generally less potent source of inhibitors than flavonoid aglycones.

Similarly, the truxinic acid derivatives junhybridins A and B (**1**, **2**) exhibited measurable inhibition, but the molecular basis of their α-glucosidase inhibition cannot be determined from the present data. To date, very limited information is available regarding the AGI activity of cyclobutane-containing truxinic acid derivatives, making direct comparison with the literature difficult [2]. Their relatively modest activity may reflect the lack of the extended conjugated aromatic system that characterizes more potent flavonoid inhibitors and facilitates interactions with the enzyme active site. Further enzyme-kinetic, molecular docking, or biophysical studies would therefore be required to clarify the binding mode and mechanism of inhibition of these compounds.

The markedly lower IC_{50} value of acarbose (0.00180 µM) compared with the isolated compounds is consistent with its established use as an α-glucosidase inhibitor. However, because assay conditions substantially influence α-glucosidase inhibition data, the present comparison should be interpreted primarily within the experimental system used in this study rather than in relation to values reported from different assay systems.

Overall, the investigated phenolic constituents displayed markedly different α-glucosidase inhibitory profiles. Luteolin (**6**) was clearly the most potent inhibitor, with an IC_{50} value of 5.91 µM, while juncusol (**4**) showed substantial inhibition at 100 µM. The newly identified junhybridins A (**1**) and B (**2**) and the other tested constituents exhibited measurable effects under the applied assay conditions. The observed differences may be related to structural characteristics of the compounds, including the hydroxylation and glycosylation patterns of flavonoids and the substitution patterns of phenanthrene and truxinic acid derivatives. However, these structural features should be considered possible explanations rather than experimentally demonstrated determinants of α-glucosidase inhibition, as no enzyme-kinetic or binding studies were performed in the present work. Taken together, the phytochemical and pharmacological results demonstrate that *J. hybridus* contains a chemically diverse set of secondary metabolites and identify luteolin as the most promising α-glucosidase inhibitor among the isolated compounds, while also providing preliminary evidence for the activity of less-studied phenanthrene and truxinic acid derivatives.

3. Materials and Methods

3.1. General Experimental Procedures

A Shimadzu UV-1800 spectrophotometer (Shimadzu Europa GmbH, Duisburg, Germany) was used to obtain UV spectra. NMR spectra were recorded in methanol-d_4 on a Bruker Avance DRX 500 spectrometer (Bruker, Ettlingen, Germany) at 500 MHz (^{1}H) and 125 MHz (^{13}C). The signal of the deuterated solvent was taken as a reference. The chemical shift values (δ) were given in ppm and coupling constants (J) are in Hz. Two-dimensional (2D) experiments were performed with standard Bruker software TopSpin 4.5.0 (bruker.com). In the ^{1}H–^{1}H COSY, NOESY, HSQC, and HMBC experiments, gradient-enhanced versions were used. The high-resolution MS spectra were acquired on a Thermo Scientific Q-Exactive Plus Orbitrap mass spectrometer (Thermo Fisher Scientific, Waltham, MA, USA) equipped with an ESI ion source in the positive or negative ionization mode. Data acquisition was performed using Thermo Scientific Xcalibur software (version 4.5.474.0; Thermo Fisher Scientific, Waltham, MA, USA). HPLC was carried out on a Shimadzu HPLC (Shimadzu LC20; Shimadzu Europa GmbH, Duisburg, Germany), using reversed-phase (Phenomenex, Kinetex Phenyl-Hexyl, 5 µm 100 A, 150 × 4.6 mm and Phenomenex, Kinetex C18, 5 µm 100 A, 150 × 4.6 mm) columns. Vacuum liquid chromatography (VLC) was carried out on silica gel (silica gel GF_{254}, 15 µm, Merck, Darmstadt, Germany). Sephadex LH-20 (25–100 µm, Sigma-Aldrich, Budapest, Hungary) was used for gel filtration. Preparative thin-layer chromatography (prep. TLC) was performed on reversed-phase silica gel plates (TLC silica gel 60 RP-18 F_{254}, Merck, Darmstadt, Germany). All solvents used in this work were of at least analytical grade (VWR Ltd., Szeged, Hungary).

3.2. Plant Material

J. hybridus Brot. (whole plant, 325 g) was grown by László Bakacsy at the Department of Plant Biology, University of Szeged, Szeged, Hungary. A voucher specimen (No. 900/2) has been deposited at the Institute of Pharmacognosy, University of Szeged, Szeged, Hungary. Seeds of *J. hybridus* were collected in May 2019 from the Larnaca Salt Lake, Cyprus (GPS coordinates: N34°53′26.05″ E33°37′45.52″). Botanical identification and collection of the plant material were performed by László Bakacsy, and a voucher specimen (No. 900/1) has

been deposited at the Institute of Pharmacognosy, University of Szeged, Szeged, Hungary). Subsequently, Florimo universal potting soil (Matécsa Gardening Ltd., Kecel, Hungary) was used for seed germination and plant cultivation. The substrate had a pH of 6.4 ± 0.5, an organic matter content of 70% (*w*/*w*), K_2O content of 0.3% (*w*/*w*) (min. 3000 mg kg^{-1}), P_2O_5 content of 0.1% (*w*/*w*) (min. 1000 mg kg^{-1}), and N content of 1.0% (*w*/*w*) (min. 10,000 mg kg^{-1}). To achieve an appropriate soil structure, sand was mixed into the potting soil at a ratio of 20%. Plants were irrigated weekly with sufficient distilled water to ensure that their trays always contained standing water. After transplantation, plants were grown in a greenhouse under a 12-h photoperiod, with day/night temperatures of 24/22 °C and a relative humidity of 55–65%. Light intensity at plant height was 300 µmol m^{-2} s^{-1}.

3.3. Extraction and Isolation

The dried and ground plant of *J. hybridus* (325 g) was extracted at room temperature with methanol (10 L) through percolation. The crude methanolic extract was concentrated (25.6 g) under reduced pressure. After evaporation, the extract was dissolved in 50% aqueous methanol, and solvent–solvent partitions were performed with *n*-hexane (10 × 0.3 L), chloroform (6 × 0.3 L), and ethyl acetate (7 × 0.3 L), respectively.

The concentrated chloroform-soluble fraction (3.0 g) was chromatographed by VLC on silica gel with a gradient system of cyclohexane–EtOAc–MeOH [from 98:2:0 to 1:1:1 (1 L/eluent), and finally with MeOH; volume of collected fractions was 100 mL], to yield eight main fractions (C/1-8). The fractions were combined based on TLC analysis using UV light at 254 and 366 nm, and visualized with vanillin sulfuric acid reagent followed by heating at 110 °C for 1 min. Fraction C/4 and C/7 were pure and afforded compound **3** (6.0 mg) from C/4 and compound **5** (40.2 mg) from C/7.

Fraction C/3 (7.2 mg) was purified by RP-HPLC under gradient conditions using MeOH–H_2O (from 6:4 to 1:0 in 7 min; flow rate 1 mL/min) as a mobile phase to yield compound **4** (0.9 mg, t_R = 6.10 min). The separation of fraction C/6 (30.6 mg) was performed by RP-HPLC under gradient conditions using MeOH–H_2O (from 35:65 to 5:5 in 7.2 min; flow rate 1 mL/min) as a mobile phase to obtain three subfractions. Fractions C/6/1 and C/6/2 were pure and yielded compound **11** (2.4 mg, t_R = 5.39 min) from C/6/1 and compound **13** (5.6 mg, t_R = 6.13 min) from C/6/2. Fraction C/6/3 (5.2 mg) was further separated by RP-HPLC using an isocratic MeOH–H_2O (3:7) eluent, at a flow rate of 1 mL/min, to yield compounds **14** (1.0 mg, t_R = 11.3 min) and **12** (1.5 mg, t_R = 12.73 min). Fraction C/8 (220.8 mg) was further separated through gel chromatography on a Sephadex LH-20 stationary phase using CH_2Cl_2–MeOH (1:1) as an eluent (C/8/1-10). Fraction C/8/3 was pure and yielded compound **15** (57.9 mg). Purification of fraction C/8/2 (42.3 mg) was performed by prep. TLC on RP silica gel using MeOH−H_2O (8:2) as a mobile phase. Subfraction C/8/2/1 (18.5 mg) was further purified by RP-HPLC under gradient conditions, using MeOH–H_2O (from 35:65 to 6:4 in 7.5 min; flow rate 1 mL/min) as a mobile phase. Subfraction C/8/2/1/1 (6.5 mg) was further separated by RP-HPLC using an isocratic MeOH–H_2O (2:8) eluent, at a flow rate of 1 mL/min, to yield compound 10 (2.5 mg, t_R = 16.85 min).

The concentrated ethyl acetate-soluble fraction (2.7 g) was separated by VLC on silica gel with a gradient system of $CHCl_3$–MeOH [from 1:0 to 1:1 (500 mL/eluent), and finally with MeOH; volume of collected fractions was 100 mL]. According to the TLC patterns, the fractions were combined to 10 main fractions (E/1-10). Fraction E/1-3 (154.8 mg, 49.9 mg, and 59.8 mg, respectively) contained compound 6 (255.3 mg).

Fraction E/5 (458.0 mg) was purified through Sephadex LH-20 gel chromatography using MeOH as an eluent. Fraction E/5/3 (311.8 mg) was further separated by reversed-phase (RP)-HPLC under gradient conditions, using MeOH–H_2O (from 2:8 to 4:6 in 3.5 min

and to 8:2 in 8.5 min; flow rate 0.8 mL/min) as a mobile phase, to yield compound **1** (290 mg, t_R = 8.88 min). Fractions E/7-10 (135.2 mg, 214.8 mg, 639.4 mg, and 452.3 mg, respectively) were purified by Sephadex LH-20 gel chromatography using CH_2Cl_2–MeOH (1:1) and 0.01% trifluoracetic acid as an eluent. Fraction E/7/2 (23.7 mg) was separated by RP-HPLC, using a MeOH–H_2O gradient solvent system (from 4:6 to 8:2 in 8.5 min; flow rate 1 mL/min) as a mobile phase, to yield compound 9 (7.6 mg t_R = 6.18 min). Fraction E/8/3 (402.5 mg) was purified by RP-HPLC, using a MeOH–H_2O gradient solvent system (from 4:6 to 7:3 in 5.5 min; flow rate 1 mL/min) as a mobile phase, to yield compound 2 (301.5 mg, t_R = 5.82 min). Purification of fraction E/8/4 (130.3 mg) was performed by RP-HPLC using MeOH–H_2O (4:6), at a flow rate of 1 mL/min, to yield compounds 7 (67.3 mg, t_R = 6.39 min) and **8** (9.4 mg, t_R = 10.15 min).

Compound **1**. Yellow solid; UV (MeOH) λ_{max} (log ε) = 207 (4.73), 233 (4.12), 282 (3.51), 322 (2.98) nm; ^{1}H and ^{13}C NMR data, see Table 1; (+)-HRESIMS *m*/*z* 754.2539 [M + NH_3 + H]$^+$, calcd for $C_{34}H_{44}O_{18}N^+$ 754.2553, Δ = −1.9 ppm.

Compound **2**. Yellow syrup; ^{1}H and ^{13}C NMR data, see Table 1; (+)-HRESIMS *m*/*z* 712.2443 [M + NH_3 + H]$^+$, calcd for $C_{32}H_{42}O_{17}N^+$, 712.2452, Δ = −1.3 ppm.

(*Z*)-2-(2,4-dihydroxy-2,6,6-trimethylcyclohexylidene)acetic acid (**13**): ^{1}H NMR (500 MHz, MeOH-d_4) δ 5.75 (1H, s, H-7), 4.21 (1H, quint, *J* = 3.5 Hz, H-4), 2.42 (1H, dt, *J* = 13.7, 2.5 Hz, H-3eq), 1.99 (1H, dt, *J* = 14.4, 2.5 Hz, H-5 eq), 1.76 (3H, s, 2-CH_3), 1.75 (1H, dd, *J* = 11.9, 4.0 Hz, H-3 ax), 1.53 (1H, dd, *J* = 14.4, 3.7 Hz, H-5 ax), 1.47 (3H, s, 6-CH_3 ax), 1.28 (3H, s, 6-CH_3 eq); ^{13}C NMR (125 MHz, MeOH-d_4) δ 185.7 (C-1), 174.4 (C-8), 113.3 (C-7), 89.0 (C-2), 67.2 (C-4), 48.0 (C-5), 46.5 (C-3), 37.2 (C-6), 31.0 (CH_3-6 eq), 27.4 (CH_3-2), 27.0 (CH_3-6 ax).

3.4. Alkaline Hydrolysis of 1 and 2

Compounds (1: 3.0 mg and 2: 3.5 mg) were hydrolyzed with 3% KOH/MeOH (3 mL) at room temperature for 15 min. The reaction mixture was neutralized with 2N HCl (monitored with indicator paper) and filtered. The filtrate was concentrated in vacuo to give a residue that was chromatographed over Sephadex LH-20 eluted with MeOH and prep. normal-phase HPLC on a LiChrospher Si60 column (5 µm, 250 × 4 mm) ($CHCl_3$/MeOH/H_2O, 9:7:1.5) to afford the aglycon and sucrose (1.0 mg from **1**; 1.3 mg from **2**). The sucrose was identified by comparison of its optical rotation value [α^{25}_D] + 25.0 (*c* 0.1, MeOH) and by co-TLC with an authentic sample using $CHCl_3$/MeOH/H_2O (9:7:1.5) as a developing system (Rf = 0.35).

3.5. α-Glucosidase Inhibition Assay

The α-glucosidase inhibition assay was performed following the methodology described by Suhail et al. [48]. A pH = 6.8 potassium phosphate buffer (0.1 M) was prepared to be used as a medium. Samples were first dissolved in DMSO (6.4 mM) and diluted with buffer to get the appropriate concentrations in the well during the reaction. On a 96-well plate, 20 µL of α-glucosidase enzyme (from *Saccharomyces cerevisiae*, 1 unit/mL in buffer) (HY-P2802, MedChemExpress, Monmouth Junction, NJ, USA) was added to 120 µL of sample solution, and the mixture was incubated at 37 °C for 15 min. The reaction was initiated through the addition of 20 µL of the substrate (5 mM para-nitrophenyl-α-D-glucopyranoside in buffer). After 15 min of incubation at 37 °C, the reaction was stopped through the addition of 80 µL of 0.2 M Na_2CO_3 in buffer. As enzyme control, an appropriate amount of DMSO in the buffer was used. The absorbance was measured using a BMG Labtech FluoStar Optima plate reader at 405 nm. The activity of the compounds was calculated as inhibition (%) = ($A_{enzyme\text{-}control}$ − A_{sample})/$A_{enzyme\text{-}control}$ × 100, where A_{sample} is the absorbance in the presence of each sample and $A_{enzyme\text{-}control}$ is the absorbance without any inhibitors,

and IC_{50} values were calculated using GraphPad Prism 10.3.1 (Dose–response—Inhibition, log(inhibitor) vs. response—variable slope (four parameters)). Results were calculated as mean ± standard deviation, without comparative statistics. Acarbose was used as a positive control, and due to its very low IC_{50} value an additional, independent experiment was performed. The dose–response curves of luteolin (**6**) and acarbose can be found in the Supplementary Materials, Figure S17. All measurements were done in technical triplicates. In the case of the flavonoids, the initial screening showed unreasonable results, indicating supposed increased activity. Under alkaline conditions, flavonoids are known to undergo a bathochromic shift, resulting in a change in color and absorption at 405 nm [49,50]; this was corrected by subtracting their own absorbance without the substrate, measured in the same alkaline conditions. Such behavior was not observed in the case of the other compounds.

4. Conclusions

The present study provides a comprehensive phytochemical characterization of *Juncus hybridus* and expands the known chemical diversity of the Juncaceae family. Two new truxinic acid sucrose esters, junhybridins A (1) and B (2), together with thirteen previously known compounds belonging to different structural classes, were identified from the whole plant. The occurrence of truxinic acid derivatives in *J. hybridus* represents a previously unreported feature within the Juncaceae family.

The isolated compounds also exhibited enzyme inhibitory activities in the in vitro assays performed in this study, providing preliminary evidence of their biological activity. However, further studies, including detailed pharmacological investigations and in vivo evaluation, are required to determine the biological significance and potential applications of the identified compounds.

Supplementary Materials: The following supporting information can be downloaded at: https://www.mdpi.com/article/10.3390/ph19111670/s1, Figure S1: (+)-HRESIMS of compound **1**; Figure S2: ^{1}H NMR spectrum of compound **1**; Figure S3. ^{13}C NMR JMOD spectrum of compound **1**; Figure S4. ^{1}H–^{1}H COSY spectrum of compound **1**; Figure S5. HSQC spectrum of compound **1**; Figure S6. HMBC spectrum of compound **1**; Figure S7. Enlarged details of the HMBC spectrum of compound **1**; Figure S8. NOESY spectrum of compound **1**; Figure S9. (+)-HRESIMS of compound **2**; Figure S10. ^{1}H NMR spectrum of compound **2**; Figure S11. ^{13}C NMR JMOD spectrum of compound **2**; Figure S12. ^{1}H–^{1}H COSY spectrum of compound **2**; Figure S13. HSQC spectrum of compound **2**; Figure S14. HMBC spectrum of compound **2**; Figure S15. Enlarged details of the HMBC spectrum of compound **2**; Figure S16. NOESY spectrum of compound **2**; Figure S17: Dose–effect curve of luteolin and control acarbose.

Author Contributions: Conceptualization, A.V.; methodology, A.V.; software, G.G.; investigation, A.B., and G.G.; resources, J.H.; data curation, A.B., and G.G.; writing—original draft preparation, A.B. and A.V.; writing—review and editing, A.V. and J.H.; supervision, J.H.; project administration, A.V.; funding acquisition, A.V. and J.H. All authors have read and agreed to the published version of the manuscript.

Funding: This research received no external funding.

Institutional Review Board Statement: Not applicable.

Informed Consent Statement: Not applicable.

Data Availability Statement: The original contributions presented in this study are included in the article/Supplementary Materials. Further inquiries can be directed to the corresponding author.

Acknowledgments: The authors are grateful to László Bakacsy (Department of Plant Biology, University of Szeged, 6726 Szeged, Hungary) for growing and collecting *J. hybridus*. The authors also acknowledge the support of the University of Szeged Open Access Fund (Grant ID: 9195).

Conflicts of Interest: The authors declare no conflicts of interest.

References

1. Tachibana, S.; Ohkubo, K.; Towers, G.H.N. 4,4′-Dihydroxytruxillic acid as a component of the cell walls of the bamboo *Phyllostachys edulis*. *Phytochemistry* **1992**, *31*, 81–83. [CrossRef]
2. Yuan, X.; Men, L.; Liu, Y.; Qui, Y.; He, C.; Huang, W. Truxillic and truxinic acid derivatives: Configuration, source, and bioactivities of natural cyclobutane dimers. *J. Holist. Integr. Pharm.* **2020**, *1*, 48–69. [CrossRef]
3. Krauze-Baranowska, M. Truxillic and truxinic acids-occurence in plant kingdom. *Acta Pol. Pharm.* **2002**, *59*, 403–410.
4. Dimberg, L.H.; Andersson, R.E.; Gohil, S.; Bryngelsson, S.; Lundgren, L.N. Identification of a sucrose diester of a substituted β-truxinic acid in oats. *Phytochemistry* **2001**, *56*, 843–847. [CrossRef]
5. Wang, N.; Yao, X.; Ishii, R.; Kitanaka, S. Bioactive sucrose esters from *Bidens parviflora*. *Phytochemistry* **2003**, *62*, 741–746. [CrossRef]
6. Lee, D.Y.; Han, K.M.; Song, M.C.; Lee, D.G.; Rho, Y.D.; Baek, N.I. A new lignan glycoside from the rhizomes of *Imperata cylindrica*. *J. Asian Nat. Prod. Res.* **2008**, *10*, 299–302. [CrossRef]
7. Liu, X.; Zhang, B.F.; Yang, L.; Chou, G.-X.; Wang, Z.-T. Four new compounds from *Imperata cylindrica*. *J. Nat. Med.* **2014**, *68*, 295–301. [CrossRef]
8. Hong, S.S.; Choi, C.W.; Choi, Y.H.; Oh, J.S. Coixlachryside A: A new lignan glycoside from the roots of *Coix lachryma jobi* L. var. *ma-yuen* Stapf. *Phytochem. Lett.* **2016**, *17*, 152–157. [CrossRef]
9. Ban, N.K.; Truong, L.H.; Tiep, T.V.; Yen, D.T.H.; Doan, V.V.; Nhiem, N.X.; Seo, Y.; Namkung, W.; Kim, S.H.; Tai, B.H.; et al. Four new sucrose diesters of substituted truxinic acids from *Trigonostemon honbaensis* with their anoctamin-1 inhibitory activity. *Bioorg. Chem.* **2020**, *102*, 104158. [CrossRef]
10. Ban, N.K.; Tai, B.H.; Thu, V.K.; Kiem, P.H. New truxinic and truxillic acid sucrose diesters from the leaves of *Trigonostemon honbaensis*. *Nat. Prod. Commun.* **2021**, *16*, 1934578X21999148. [CrossRef]
11. Deepa, V.S.; Rajaram, K.; Sureshkumar, P. Dimethyl 3,3′,4,4′-tetrahydroxy-δ-truxinate isolated from the leaves of *Andrographis lineata* Wall. ex. Nees suppress adipogenesis in 3T3-L1 preadipocytes for type 2 diabetes. *Pak. J. Pharm. Sci.* **2015**, *28*, 443–448. [CrossRef]
12. Morikawa, T.; Ninomiya, K.; Akaki, J.; Kakihara, N.; Kuramoto, H.; Matsumoto, Y.; Hayakawa, T.; Muraoka, O.; Wang, L.-B.; Wu, L.-J.; et al. Dipeptidyl peptidase-inhibitory activity of dimeric dihydrochalcone glycosides from flowers of *Helichrysum arenarium*. *J. Nat. Med.* **2015**, *69*, 494–506. [CrossRef]
13. Liang, D.; Liu, Y.-F.; Hao, Z.-Y.; Luo, H.; Wang, Y.; Zhang, C.-L.; Chen, R.-Y.; Yu, D.-Q. Acylated flavonol glycosides and δ-truxinate derivative from the aerial parts of *Lysimachia clethroides*. *Phytochem. Lett.* **2015**, *11*, 116–119. [CrossRef]
14. El-Shamy, A.I.; Abdel-Razek, A.F.; Nassar, M.I. Phytochemical review of *Juncus* L. genus (Fam. Juncaceae). *Arab. J. Chem.* **2012**, *8*, 614–623. [CrossRef]
15. Bús, C.; Tóth, B.; Stefkó, D.; Hohmann, J.; Vasas, A. Family Juncaceae: Promising source of biologically active natural phenanthrenes. *Phytochem. Rev.* **2018**, *17*, 833–851. [CrossRef]
16. Della Greca, M.; Fiorentino, A.; Monaco, P.; Previtera, L.; Zarrelli, A. Effusides I-V: 9,10-dihydrophenanthrene glucosides from *Juncus effusus*. *Phytochemistry* **1995**, *40*, 533–535. [CrossRef]
17. Tóth, B.; Hohmann, J.; Vasas, A. Phenanthrenes: A promising group of plant secondary metabolites. *J. Nat. Prod.* **2018**, *81*, 661–678. [CrossRef]
18. Bús, C.; Kúsz, N.; Jakab, G.; Tahaei, S.A.S.; Zupkó, I.; Endrész, V.; Bogdanov, A.; Burián, K.; Csupor-Löffler, B.; Hohmann, J.; et al. Phenanthrenes from *Juncus compressus* Jacq. with promising antiproliferative and anti-HSV-2 activities. *Molecules* **2018**, *23*, 2085. [CrossRef]
19. Stefkó, D.; Kúsz, N.; Szemerédi, N.; Barta, A.; Spengler, G.; Berkecz, R.; Hohmann, J.; Vasas, A. Unique phenanthrenes from *Juncus ensifolius* and their antiproliferative and synergistic effects with the conventional anticancer agent doxorubicin against human cancer cell lines. *Pharmaceutics* **2022**, *14*, 608. [CrossRef]
20. De Natale, A.; Pollio, A.; De Marco, A.; Luongo, G.; Di Fabio, G.; Zarrelli, A. Phenanthrene dimers: Promising source of biologically active molecules. *Curr. Top. Med. Chem.* **2022**, *22*, 939–956. [CrossRef]
21. Sahuc, M.E.; Sahli, R.; Rivière, C.; Pène, V.; Lavie, M.; Vandeputte, A.; Brodin, P.; Rosenberg, A.R.; Dubuisson, J.; Ksouri, R.; et al. Dehydrojuncusol, a natural phenanthrene compound extracted from *Juncus maritimus*, is a new inhibitor of Hepatitis C virus RNA replication. *J. Virol.* **2019**, *93*, e02009–18. [CrossRef]
22. Ngan, T. Bioactive compounds in anti-diabetic plants: From herbal medicine to modern drug discovery. *Biology* **2020**, *9*, 252. [CrossRef]
23. Annapurna, H.V.; Babu, A.; Natesan, R.; Arun, K.P.; Brindha, P.; Sethuraman, S.; Mahadevan, V.; Nagarajan, A. Isolation and in silico evaluation of antidiabetic molecules of *Cynodon dactylon* (L.). *J. Mol. Graph. Model.* **2012**, *39C*, 87–97. [CrossRef]

24. Hyder, A. Naturally-occurring carboxylic acids from traditional antidiabetic plants as potential pancreatic islet FABP3 inhibitors. A molecular docking–aided study. *Chem. Biol. Interact.* **2023**, *372*, 110368. [CrossRef]
25. Hao, Z.-Y.; Wang, X.; Yang, M.; Zhou, S.-Q.; Xiao, C.-Y.; Zhang, J.-Y.; Xie, S.-S.; Li, M.; Cao, Y.-G.; Sun, Y.-J.; et al. In vitro anti-diabetic activities of phytochemicals isolated from *Cornus officinalis* fruits. *Fitoterapia* **2026**, *188*, 106984. [CrossRef]
26. San, H.T.; Chatsumpun, N.; Juengwatanatrakul, T.; Pornputtapong, N.; Likhitwitayawuid, K.; Sritularak, B. Four novel phenanthrene derivatives with α-glucosidase inhibitory activity from *Gastrochilus bellinus*. *Molecules* **2021**, *26*, 418. [CrossRef]
27. Lam, T.P.; Tran, N.N.; Pham, L.D.; Lai, N.V.; Dang, B.N.; Truong, N.N.; Nguyen-Vo, S.K.; Hoang, T.L.; Mai, T.T.; Tran, T.D. Flavonoids as dual-target inhibitors against α-glucosidase and α-amylase: A systematic review of in vitro studies. *Nat. Prod. Bioprospect.* **2024**, *14*, 4. [CrossRef]
28. Takahashi, T.; Miyazawa, M. Synthesis and structure–activity relationships of serotonin derivatives effect on α-glucosidase inhibition. *Med. Chem. Res.* **2012**, *21*, 1762–1770. [CrossRef]
29. Barta, A.; Petz, P.; Bakacsy, L.; Hohmann, J.; Vasas, A. Phytochemical investigation of cultivated *Juncus hybridus*. 5th Symposium of Young Researchers on Pharmacognosy, Szeged, Hungary, 23 July 2024.
30. Kim, K.H.; Chang, S.W.; Lee, K.R. Feruloyl sucrose derivatives from *Bistorta manshuriensis*. *Can. J. Chem.* **2010**, *88*, 519–523. [CrossRef]
31. Della Greca, M.; Fiorention, A.; Mangoni, L.; Monaco, P.; Previtera, L. 9,10-dihydrophenanthrene metabolites from *Juncus effusus* L. *Tetrahedron Lett.* **1992**, *33*, 5257−5260. [CrossRef]
32. Shen, C.C.; Chang, Y.S.; Ho, L.K. Nuclear magnetic resonance studies of 5,7-dihydroxyflavonoids. *Phytochemistry* **1993**, *34*, 843−845. [CrossRef]
33. Xu, T.; Wang, C.; Jiang, S.; Yang, T.; Wu, X. Glycosylation of luteolin in hydrophilic organic solvents and structure–antioxidant relationships of luteolin glycosides. *RSC Adv.* **2022**, *12*, 18232–18237. [CrossRef]
34. Schwaiger, S.; Seger, C.; Wiesbauer, B.; Schneider, P.; Ellmerer, E.P.; Sturm, S.; Hermann, S. Development of an HPLC-PAD-MS assay for the identification and quantification of major phenolic edelweiss (*Leontopodium alpium* Cass.) constituents. *Phytochem. Anal.* **2006**, *17*, 291–298. [CrossRef]
35. Hammami, S.; Jannet, H.B.; Bergaoui, A.; Ciavatta, L.; Cimino, G.; Mighri, Z. Isolation and structure elucidation of a flavanone, a flavanone glycoside and vomifoliol from *Echiochilon fruticosum* growing in Tunisia. *Molecules* **2004**, *9*, 602–608. [CrossRef]
36. Kai, H.; Bata, M.; Okuyama, T. Two new megastigmanes from the leaves of *Cucumis sativus*. *Chem. Pharm. Bull.* **2007**, *55*, 133−136. [CrossRef]
37. Kim, I.; Chin, Y.-W.; Li, S.W.; Kim, Y.C.; Kim, J. Norisoprenoids and hepatoprotective flavone glycosides from the aerial parts of *Beta vulgaris* var. *cicla*. *Arch. Pharm. Res.* **2004**, *27*, 600–603. [CrossRef]
38. Wu, Y.; Su, J.; Guo, R.; Ren, T.; Zhang, M.; Dong, M.; Sauriol, F.; Shi, Q.; Gu, Y.; Huo, C. Two new non-taxoids from leaves of *Taxus cuspidata*. *Chem. Nat. Comp.* **2014**, *50*, 603–605. [CrossRef]
39. Luo, J.; Li, L.; Kong, L. Preparative separation of phenylpropenoid glycerides from the bulbs of *Lilium lancifolium* by high-speed counter-current chromatography and evaluation of their antioxidant activities. *Food Chem.* **2012**, *131*, 1056–1062. [CrossRef]
40. Chen, X.-L.; Zhang, K.; Zhao, X.; Wang, H.-L.; Han, M.; Li, R.; Zhang, Z.-N.; Zhang, Y.-M. Triterpenoids from Kochiae fructus: Glucose uptake in 3T3-L1 adipocytes and α-glucosidase inhibition, in silico molecular docking. *Int. J. Mol. Sci.* **2023**, *24*, 2454. [CrossRef]
41. Dirir, A.M.; Daou, M.; Yousef, A.F.; Yousef, L.F. A review of alpha-glucosidase inhibitors from plants as potential candidates for the treatment of type-2 diabetes. *Phytochem. Rev.* **2022**, *21*, 1049–1079. [CrossRef]
42. Wang, R.Y.; Su, P.J.; Li, B.; Zhan, X.Q.; Qi, F.M.; Lv, C.W.; Hu, F.D.; Gao, K.; Zhang, Z.X.; Fei, D.Q. Two new aromatic derivatives from *Codonopsis pilosula* and their α-glucosidase inhibitory activities. *Nat. Prod. Res.* **2022**, *36*, 4929–4935. [CrossRef]
43. Le, T.M.; Nguyen, H.N.; Vu, N.T.; Le, P.Q. Synthesis and biological evaluation of diastereomeric natural products: Discovery of a novel synergistic combination for α-glucosidase inhibition. *Bioorg. Med. Chem. Lett.* **2025**, *123*, 130239. [CrossRef]
44. Yan, J.; Zhang, G.; Pan, J.; Wang, Y. α-Glucosidase inhibition by luteolin: Kinetics, interaction and molecular docking. *Int. J. Biol. Macromol.* **2014**, *64*, 213–223. [CrossRef]
45. Lee, J.Y.; Lee, H.S.; Lee, Y.Y.; Kim, M.-H.; Kim, H.-J.; Han, N.; Kang, M.S.; Yeon, Y.J. Comprehensive study on the inhibition mechanism of alpha-glucosidase by flavonoids via kinetic and structural analysis. *Biotechnol. Bioproc. E* **2024**, *29*, 413–425. [CrossRef]
46. Şöhretoğlu, D.; Renda, G.; Arroo, R.; Xiao, J.; Sari, S. Advances in the natural α-glucosidase inhibitors. *eFood* **2023**, *4*, e112. [CrossRef]
47. Kim, J.S.; Kwon, C.S.; Son, K.H. Inhibition of alpha-glucosidase and amylase by luteolin, a flavonoid. *Biosci. Biotechnol. Biochem.* **2000**, *64*, 2458–2461. [CrossRef]
48. Suhail, P.; Joy, J.; Musliyarakath, N.; Padmaraj, C.P.; Theruvath, A.; Varghese, N. Bioactive compounds from *Carica papaya* (papaya) fruit peel target key enzymes in diabetes and dyslipidemia: A molecular insight. *Biomed. Biotechnol. Res. J.* **2025**, *9*, 246–254. [CrossRef]

49. Waterman, P.G.; Mole, S. *Analysis of Phenolic Plant Metabolites*; Blackwell Scientific Publications: Oxford, UK, 1994.
50. Álvarez-Diduk, R.; Ramírez-Silva, M.T.; Galano, A.; Merkoçi, A. Deprotonation mechanism and acidity constants in aqueous solution of flavonols: A combined experimental and theoretical study. *J. Phys. Chem. B* **2013**, *117*, 12347–12359. [CrossRef]

Disclaimer/Publisher's Note: The statements, opinions and data contained in all publications are solely those of the individual author(s) and contributor(s) and not of MDPI and/or the editor(s). MDPI and/or the editor(s) disclaim responsibility for any injury to people or property resulting from any ideas, methods, instructions or products referred to in the content.